

Growth dynamics of pentacene thin films: Real-time synchrotron x-ray scattering study

Alex C. Mayer,¹ Ricardo Ruiz,^{1,*} Hua Zhou,² Randall L. Headrick,² Alexander Kazimirov,³ and George G. Malliaras^{1,†}

¹*Materials Science and Engineering, Cornell University, Ithaca, New York 14853, USA*

²*Department of Physics, University of Vermont, Burlington, Vermont 05405, USA*

³*Cornell High Energy Synchrotron Source, Ithaca, New York 14853, USA*

(Received 28 March 2006; published 4 May 2006)

Real-time synchrotron x-ray scattering in the anti-Bragg configuration was used to monitor the dynamics of pentacene film growth on inert substrates. A distributed-growth model, according to which pentacene molecules adsorbed on the n th layer can either nucleate and contribute to the growth of the $(n+1)$ th layer or transfer downward and contribute to the growth of the n th layer, gave a good description of the data. For molecules adsorbed on the first and second layers, the probability of downward transfer was found to be dependent on the substrate, and independent of temperature within the range from 25 to 60 °C. For films grown on SiO₂, an Ehrlich-Schwoebel barrier of the order of 70 meV dominated downward transfer of pentacene molecules in layers away from the substrate. For films grown on an alkylated self-assembled monolayer, significant desorption of pentacene molecules from the substrate at elevated temperatures forced the growth mode toward the three-dimensional limit.

DOI: [10.1103/PhysRevB.73.205307](https://doi.org/10.1103/PhysRevB.73.205307)

PACS number(s): 68.55.-a, 61.10.Kw, 68.37.Ps

I. INTRODUCTION

The electronics industry relies heavily on our ability to deposit, in an extremely controlled way, thin films of inorganic materials. Such films are used in every integrated circuit like conductor lines, diffusion barriers, semiconducting channels, and gate insulators.¹ The fine control over the structure, morphology, and, ultimately, properties of these films stems from a deep fundamental understanding of the physics of inorganic thin film growth. Over the past two decades, organic semiconductors have emerged as a technologically important class of electronic materials.² Contrary to traditional inorganic electronic materials, organics are characterized by complex, covalently bonded building blocks (molecules) that are held together by weak van der Waals interactions. One such example is pentacene, which has emerged as a model organic semiconductor due to its potential for applications in organic thin film transistors.^{3,4} The growth physics of these complex materials is largely unexplored, which is a major obstacle for the development of an organic electronics technology.

A great deal of work has focused on understanding the crystal structure of organic thin films.⁵ However, relatively little attention has been devoted to film morphology. Of particular interest is the morphology of films grown on insulating substrates, as this configuration is used in organic thin film transistors.³ Layer-by-layer or two-dimensional (2D) growth, where the organic layer fully completes before the next one nucleates and begins to grow, represents the desirable growth mode for electronic devices.⁶ The other extreme is the island or 3D growth mode, where isolated islands that offer no electrical connectivity nucleate and grow. Atomic force microscopy (AFM) has emerged as the technique of choice to characterize pentacene film morphology and infer the growth mode.⁷ Ruiz *et al.*⁸ studied submonolayer nucleation and growth and found that the initial growth regime on SiO₂ was 2D. In contrast, in films grown on polymethylmethacrylate (PMMA) at elevated temperatures, the nucleation of the second layer before completion of the first layer

has been observed.⁹ In related work on pentacene, tetracene, and perylene Verlaak *et al.*¹⁰ reported a transition from 2D to 3D growth that occurred on substrates treated with self-assembled monolayers and at high substrate temperatures. It was proposed that strong interlayer interactions and weak molecule-substrate interactions favor 3D growth. Pratontep *et al.*¹¹ compared nucleation of pentacene on inorganic dielectrics and PMMA and commented on activation energies for surface diffusion and desorption.

Being able to control the morphology of an organic film ultimately involves understanding its growth dynamics, which describe the fate of a molecule as it undergoes a variety of processes such as adsorption, desorption, diffusion, nucleation, addition, and transfer between layers. Although the dynamics of pentacene growth on conducting substrates has received some attention,¹² its growth dynamics on insulating substrates remains virtually unexplored.¹³ Synchrotron x-ray scattering is a real-time, noninvasive technique that is compatible with insulating substrates and uniquely suited to probe these processes and determine their relative importance. Mayer *et al.*¹³ and Krause *et al.*¹⁴ have recently demonstrated the applicability of this technique to monitor the evolution of organic thin film morphology.

In this paper, we report on real-time synchrotron x-ray scattering in the anti-Bragg configuration that was used to monitor the growth of pentacene thin films on inert substrates. Growth was monitored for films deposited on silicon oxide and hexadecyltrichlorosilane (HTS), at 25 and 60 °C. The experiments provide additional insights into the growth of pentacene films: First, the downward transfer of pentacene molecules adsorbed on the first two monolayers is dominated by the substrate-pentacene interactions and does not depend on temperature. Second, for films grown on silicon dioxide, the downward transfer of pentacene molecules far from the substrate is dominated by an Ehrlich-Schwoebel barrier of the order of 70 meV. Third, for films grown on alkylated substrates, significant desorption of pentacene molecules from the substrate at elevated substrate temperatures drives the film growth mode toward the 3D limit.

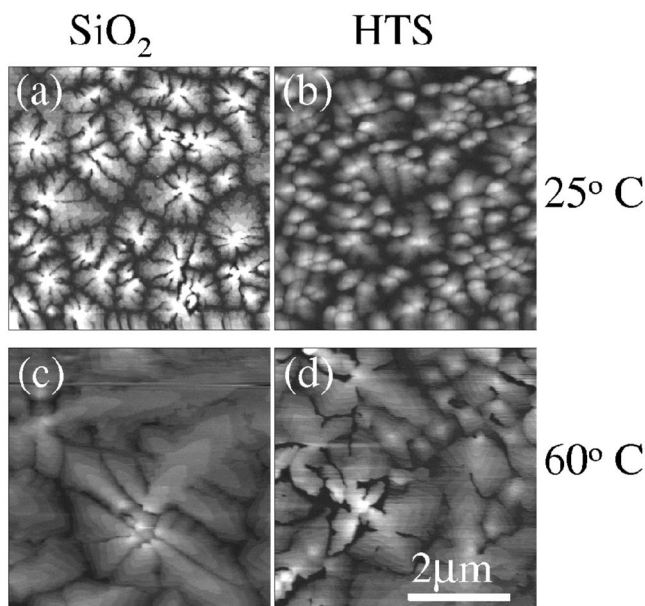


FIG. 1. AFM micrographs of ~ 7 ML thick pentacene films grown on (a) SiO₂ held at 25 °C, (b) HTS held at 25 °C, (c) SiO₂ held at 60 °C, and (d) HTS held at 60 °C.

II. EXPERIMENT

The pentacene deposition took place in a custom-built chamber (described previously^{13,15}), which was mounted at the A2 station of Cornell High Energy Synchrotron Source (CHESS) using 9.861 keV x rays to monitor *in situ* growth through Be windows. Up to seven monolayers (ML) of pentacene were deposited at a rate of 0.25 ML/min. The deposition was monitored by a quartz-crystal microbalance (passivated with pentacene) that was calibrated using AFM measurements in sub-ML thick films grown on room-temperature SiO₂. Therefore, the desorption rates discussed below should be taken as relative to growth on room-temperature SiO₂. The pressure during the deposition was of the order of 10^{-6} torr. A scintillator counter was used for measuring the scattered x-ray intensity. After deposition, AFM was conducted *ex situ* in tapping mode using a DI 3100 Dimension microscope. For the SiO₂ substrates, a 300 nm wet oxide was grown at the Cornell Nanofabrication Facility. These substrates were cleaned prior to pentacene deposition in an ultrasonic bath with deionized water and soap, dried with filtered nitrogen, and treated with uv and ozone for 10 min. For the HTS substrates, the silicon wafers with native oxide were first cleaned with a piranha etch (a H₂SO₄ and H₂O₂ mixture). The deposition of the HTS was subsequently carried out in the manner described by Vuillaume *et al.*¹⁶ The HTS-coated samples were then placed in the vacuum chamber for pentacene deposition without further cleaning.

III. RESULTS

A. Film morphology dependence on growth conditions

Figure 1 shows AFM micrographs of the films grown for

this study. The images show the characteristic pyramid-shaped grains of pentacene, with monolayer-high steps.⁷ X-ray diffraction data (not shown) verified that these films consist of the “thin film” phase only, with a spacing of $d \sim 15.4$ Å.^{7,17} In agreement with previous studies,⁷ and as expected for homogeneous nucleation, the apparent grain size of the pentacene films increases with substrate temperature. Also, at a given temperature, films grown on SiO₂ show larger grains than films grown on HTS. This has been observed before and was attributed to different wetting properties of the pentacene layers on self-assembled monolayers.^{10,18,19}

B. Anti-Bragg x-ray scattering

The x-ray scattering data were analyzed according to the kinematic approximation.²⁰ The scattered x-ray intensity for reflections normal to the surface for pentacene on an inert substrate can be described as

$$I(\Theta_{total}) = \left| r_{sub}e^{-i\phi} + r_{pent} \sum_n \theta_n e^{-iqdn} \right|^2 \quad (1)$$

where r_{sub} is the reflection amplitude of the substrate, r_{pent} is the reflection amplitude from a layer of the film, θ_n is the coverage of the n th layer of the film, Θ_{total} is the total coverage, q is the momentum transfer, d is the layer spacing of the pentacene film, and ϕ is the phase difference between the waves reflected from the substrate and from the first layer of the film. In the “anti-Bragg” configuration, q is chosen such that $qd = \pi$, and the scattered intensity is measured along the $(00\frac{1}{2})$ reflection. The scattered intensities from two adjacent layers, therefore, interact destructively with each other, and this destructive interference leads to an increased surface sensitivity that represents itself through oscillations in the intensity as material is deposited on the substrate and the individual layers nucleate and evolve.

The anti-Bragg oscillations for the four films are displayed in Fig. 2, where the scattered intensity is plotted as a function of the nominal film thickness (obtained from the quartz microbalance). Several oscillations are observed for the films grown on SiO₂, indicating that the early stages grow in a layer-by-layer fashion. Particularly telling is the presence of a cusp at a thickness of precisely one monolayer, which indicates that the first layer completes before the second layer nucleates, a fact that has been confirmed by AFM measurements.^{8,21} On the other hand, growth on HTS is characterized by a suppression of the anti-Bragg oscillations, indicating a departure from layer-by-layer growth. The lack of a sharp cusp at one monolayer indicates that the second layer nucleates well before the first layer is completed.

C. Distributed growth model

Further insight into the data was obtained by a quantitative analysis of the anti-Bragg oscillations. The solid lines in Fig. 2 are fits to Eq. (1) using a distributed model first proposed by Cohen *et al.*²² and has been successfully used to interpret the growth of a variety of materials including Ag (Ref. 23) and GaN.²⁴ This model, which provides a simple

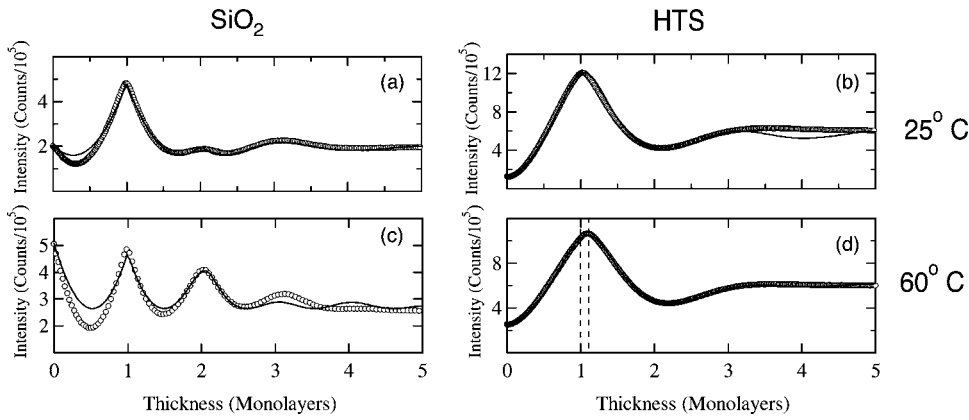


FIG. 2. Real-time anti-Bragg oscillations of the films shown in Fig. 1 plotted against the nominal thickness extracted from the quartz crystal microbalance. The solid curves are the results of fits to the distributed-growth model. The dashed lines and the arrows in (d) draw attention to the influence of desorption.

yet powerful way to analyze growth dynamics, was recently also applied with success to the growth of pentacene on silicon oxide at room temperature.¹³ Accordingly, the coverage of the n th layer is given by

$$\frac{d\theta_n}{dt} = [(\theta_{n-1} - \theta_n)(v - v_n^{des}) - v\alpha_{n-1}(\theta_{n-1} - \theta_n) + v\alpha_n(\theta_n - \theta_{n+1})] \quad (2)$$

where v is the deposition rate, v_n^{des} is the rate of desorption from the n th layer, and α_n measures the rate at which molecules transfer from the $(n+1)$ th to the n th layer. The desorption of molecules that land on a pentacene layer is neglected ($v_n^{des}=0$ for $n>1$), an assumption that is discussed below. Also, the desorption of molecules that have been captured by an island is neglected, an assumption that is validated by the observation that the morphology of pentacene films does not evolve upon heating to 60 °C and that the scattered intensity is constant if the deposition is stopped at any point in the growth (not shown). The parameters α_n can be expressed in terms of the island perimeter d_n of the n th layer as²²

$$\alpha_n = A_n \frac{d_n}{d_n + d_{n+1}} \quad (3)$$

where A_n accounts for the probability of a molecule sitting on the perimeter of the $(n+1)$ th layer to transfer downward and join the n th layer. The island perimeter of a layer is a function of the layer coverage (see Ref. 13 for methodology of data analysis), while A_n is a function of the Ehrlich-Schwoebel barrier.^{25,26} The set of A_n 's determines the growth mode and the limits of layer-by-layer and island growth are reached for $A_n=1$ and 0, respectively.²²

IV. DISCUSSION

The growth dynamics of pentacene films can be understood using different probabilities for the first (A_1), the second (A_2), and subsequent (A_{pent} for $n \geq 3$) pentacene layers. Such thickness-dependent probabilities account for the difference between substrate-pentacene and pentacene-pentacene interactions in the direction normal to the surface, and are determined empirically in heteroepitaxial systems.^{14,23} Taking $A_2 \neq A_1$ can be justified by the fact that the nucleation density for the first layer is not necessarily the

same as for subsequent layers;⁸ therefore, molecules joining the second layer see a different “substrate” from the ones joining layers number 3 and higher. The use of three independent probabilities (as opposed to a different one for each layer) allows a good fit to all the data, as seen in Fig. 2, while maintaining a minimal set of growth parameters.

The values of A_n according to a fit of Eqs. (1)–(3) to the data of Fig. 2, shown on Table I, seems to justify the choice of three independent parameters. For room-temperature growth, the probabilities to transfer downward and join the first and the second layers, A_1 and A_2 , respectively, are substrate dependent, while A_{pent} is a characteristic of pentacene and does not depend on the substrate. For growth on SiO₂, $A_1=A_2=1.0$, indicating that the early stages of growth take place in a layer-by-layer mode, as reported earlier.^{7,13} An $A_{pent}=0.6$ indicates that the growth deviates from this limit as the film grows thicker.²⁷ For growth on HTS, $A_1=0.9$ and $A_2=0.7$, indicating that the deviation from layer-by-layer growth sets in at earlier stages. The data also show A_1 and A_2 to be independent of temperature within the error of the measurement for the temperature range investigated here (see Table I). This suggests that the interaction between pentacene and the substrate dominates the mechanism of growth of the first two layers.

The parameter A_{pent} measures the probability of a molecule landing on a pentacene layer ($n \geq 3$) transferring down to the next pentacene layer. For growth on SiO₂, A_{pent} increases from 0.6 to 0.8 when the substrate temperature increases from 25 to 60 °C. Assuming that the rate-limiting step is thermal activation over the Ehrlich-Schwoebel barrier^{25,26} [$A_{pent} \sim \exp(-E_{ES}/kT)$], a barrier of $E_{ES} \approx 70$ meV is obtained. This value is a fraction of the energies

TABLE I. Probabilities for pentacene molecules to transfer downward and join the layer below for films grown on SiO₂ and HTS at two different temperatures. The error was estimated by fitting data from different runs.

| T (°C) | Substrate | A_1 | A_2 | A_{pent} |
|----------|------------------|----------|----------|------------|
| 25 | SiO ₂ | 1.0±0.01 | 1.0±0.05 | 0.6±0.1 |
| 25 | HTS | 0.9±0.05 | 0.7±0.05 | 0.6±0.1 |
| 60 | SiO ₂ | 1.0±0.01 | 1.0±0.05 | 0.8±0.1 |
| 60 | HTS | 0.9±0.05 | 0.7±0.05 | 0.4±0.1 |

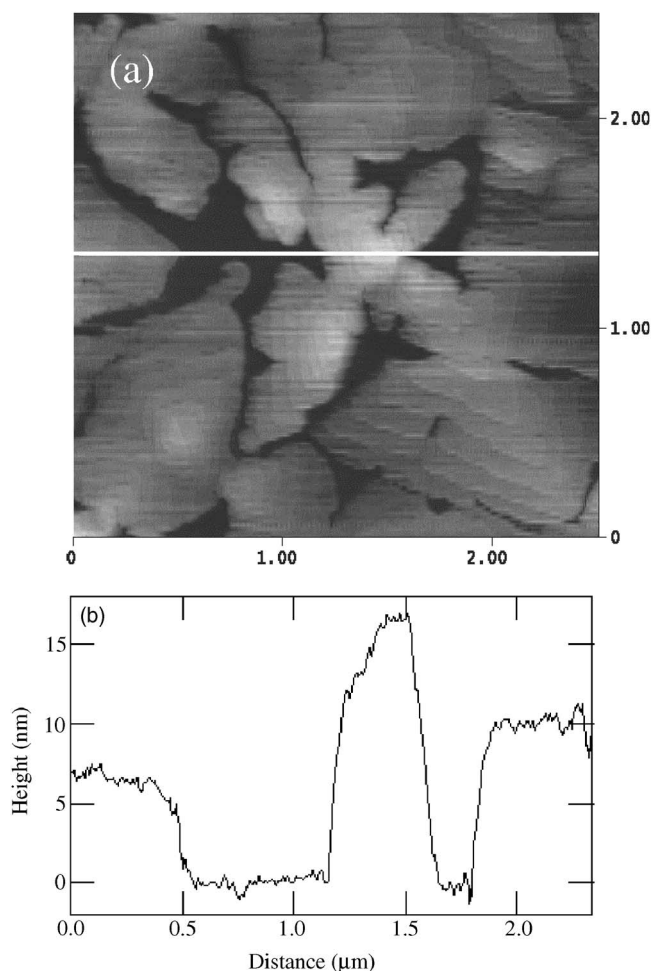


FIG. 3. (a) Close-up of the film grown on HTS at 60 °C [Fig. 1(d)], and (b) cross section [along the line in (a)] showing step heights of several monolayers.

for intralayer (of the order of 400 meV), and interlayer (of the order of 150 meV) interactions in pentacene.¹⁰ This is consistent with metals, where barriers of the order of 0.2 eV occur for bond strengths of the order of 3–4 eV.²³

On the other hand, the temperature dependence of A_{pent} for films grown on HTS is anomalous, as A_{pent} decreases from 0.6 to 0.4 when the substrate temperature increases from 25 to 60 °C. This behavior of A_{pent} is the result of a transition to 3D growth and the formation of steps that are more than one monolayer high. Such multimolecular steps arise when the step flow of layers closer to the substrate is slowed down, allowing subsequent layers to catch up.⁶ As Eq. (2) does not implicitly take into account transfer between steps that are more than one molecule high, this transition to 3D growth manifests itself by a decrease in A_{pent} . Such multimolecular steps can be directly observed by AFM. Figure 3(a) shows a close-up of the film grown on HTS at 60 °C. Deep crevices that go all the way to the substrate are visible, accompanied by step edges that are at least five monolayers high, as seen in the line scan [Fig. 3(b)].

According to the above, the mechanism responsible for this transition to 3D growth is desorption of pentacene molecules from the substrate, which slows down the flow of the

first step, allowing the second step to catch up. Since the two-monolayer step that is formed propagates at a considerably slower speed than a single-monolayer step,⁶ it becomes easier for the third step to catch up, and growth is driven toward the 3D limit. This mechanism is accentuated by the fact that $A_1 < 1$ for HTS, which reduces the supply of molecules joining the first layer from above. The role of desorption as a factor inducing a transition to 3D growth has not been discussed before to our knowledge. Krause *et al.*¹⁴ explored the temperature dependence of a 2D-3D transition in 3,4,9,10-perylene-tetracarboxylic-dianhydride (PTCDA) on Ag (111). The strong binding energy between PTCDA and the metal substrate renders desorption negligible in this system. Verlaak *et al.*¹⁰ found that the transition to 3D growth of pentacene on alkylated self-assembled monolayers (SAMs) occurred at a lower temperature than on SiO₂. This was discussed in terms of the relevant interaction energies (stronger interaction between pentacene and SiO₂ than between pentacene and alkylated SAMs), without explicitly including the effects of desorption.

The literature is not clear on the relative magnitude of desorption from SiO₂ and from organic substrates. Most studies have assumed negligible desorption of pentacene from SiO₂ at room temperature.⁷ Estimates indicate a stronger interaction between pentacene and SiO₂ than pentacene and some alkylated SAMs (Ref. 10) or PMMA,¹¹ in agreement with our findings here. However, this is at odds with recent work by Pratontep *et al.*,¹¹ who measured significant desorption from SiO₂ at room temperature. This discrepancy could be attributed to different surface treatment of the oxide. Direct evidence that desorption is more facile from HTS than from uv-ozone-cleaned SiO₂ is directly seen in the anti-Bragg data of Fig. 2. In the absence of desorption, Eq. (1) predicts a peak in the x-ray scattering at precisely 1 ML. This is the case in Figs. 2(a)–2(c), for growth on SiO₂ at 25 and 60 °C, and on HTS at 25 °C. Therefore, there is no substantial difference in pentacene desorption under these conditions. Moreover, the second peak in Figs. 2(a) and 2(c), which corresponds to the formation of a nearly complete second monolayer of pentacene, occurs at a nominal thickness of 2 ML. Since desorption of pentacene molecules from a pentacene underlayer is negligible, desorption from the substrate must be negligible under these conditions. This allowed us to set $v_1^{des} = 0$ in Eq. (2) for the data of Figs. 2(a)–2(c). However, the data for the films grown on HTS at 60 °C [Fig. 2(d)], show a peak that occurs past 1 ML, indicating that significant desorption from the substrate takes place under these conditions. A fit of Eqs. (1)–(3) to the data was only possible when v_1^{des} was set as a fit parameter and was found to be equal to 0.02 ML/min.

V. CONCLUSIONS

In conclusion, real-time synchrotron x-ray scattering in the anti-Bragg configuration was used to monitor the growth of pentacene thin films on inert substrates. A distributed-growth model, according to which pentacene molecules adsorbed on the n th layer can either nucleate and contribute to the growth of the $(n+1)$ th layer or transfer downward and

contribute to the growth of the n th layer, gave a good description of the data and provided significant insights into the growth of pentacene films. First, for molecules adsorbed on the first and second layers, the probability of downward transfer was found to be dependent on the substrate, and independent of temperature within the range from 25 to 60 °C. Second, for films grown on SiO₂, an Ehrlich-Schwoebel barrier of the order of 70 meV dominated downward transfer of pentacene molecules in layers away from the substrate. Third, for films grown on an alkylated self-assembled monolayer, significant desorption of pentacene molecules from the substrate forced the growth mode toward the 3D limit at elevated temperatures.

ACKNOWLEDGMENTS

The authors would like to thank Alex Yanson, Yuval Yaish, and Paul L. McEuen for HTS preparation, as well as Jack Blakely for fruitful discussion. This work was supported by the CCMR, a Materials Research Science and Engineering Center of the National Science Foundation (Grant No. DMR-9632275). A portion of this work was conducted at the Cornell High Energy Synchrotron Source (CHESS), which is supported by the National Science Foundation under Award No. DMR 97-13424, and at the Cornell Nanofabrication Facility (a member of the National Nanofabrication Users Network) which is supported by the National Science Foundation under Grant No. ECS-9731293.

*Present address: IBM T. J. Watson Research Laboratory, Yorktown Heights, NY 10598.

†Author to whom correspondence should be addressed. Email address: ggml@cornell.edu

¹S. O. Kasap, *Principles of Electronic Materials and Devices* (McGraw-Hill, Boston, 2002).

²G. G. Malliaras and R. H. Friend, *Phys. Today* **58** (5), 53 (2005).

³C. D. Dimitrakopoulos and P. R. L. Malenfant, *Adv. Mater.* (Weinheim, Ger.) **14**, 99 (2002).

⁴Y. Y. Lin *et al.*, *IEEE Electron Device Lett.* **12**, 606 (1997).

⁵A. Silinsh and V. Čápek, *Organic Molecular Crystals: Interaction, Localization and Transport Phenomena* (AIP, New York, 1994).

⁶I. V. Markov, *Crystal Growth for Beginners: Fundamentals of Nucleation, Crystal Growth and Epitaxy* (World Scientific, Singapore, 1995).

⁷R. Ruiz, D. Choudhary, B. Nickel, T. Toccoli, K. C. Chang, A. C. Mayer, P. Clancy, J. M. Blakely, R. L. Headrick, S. Iannotta, and G. G. Malliaras, *Chem. Mater.* **16**, 4497 (2004).

⁸R. Ruiz, B. Nickel, N. Koch, L. C. Feldman, R. F. Haglund, A. Kahn, and G. Scoles, *Phys. Rev. B* **67**, 125406 (2003).

⁹Y. Luo, G. Wang, J. A. Theobald, and P. H. Beton, *Surf. Sci.* **537**, 241 (2003).

¹⁰S. Verlaak, S. Steudel, P. Heremans, D. Janssen, and M. S. Deleuze, *Phys. Rev. B* **68**, 195409 (2003).

¹¹S. Pratontep, F. Nuesch, L. Zuppiroli, and M. Brinkmann, *Phys. Rev. B* **72**, 085211 (2005).

¹²F.-J. Meyer Zu Heringdorf, M. C. Reuter, and R. M. Tromp, *Nature* (London) **412**, 517 (2001).

¹³A. C. Mayer, R. Ruiz, R. L. Headrick, A. Kazimirov, and G. G. Malliaras, *Org. Electron.* **5**, 257 (2004).

¹⁴B. Krause, F. Schreiber, H. Dosch, A. Pimpinelli, and O. H.

Seeck, *Europhys. Lett.* **65**, 372 (2004).

¹⁵R. L. Headrick, G. G. Malliaras, A. C. Mayer, A. K. Deyhim, and A. C. Hunt, in *Eighth International Conference on Synchrotron Radiation Instrumentation*, edited by T. Warwick, H. Stohr, H. A. Padamore, and J. Arthur, AIP Conf. Proc. No. 705 (AIP, Melville, NY, 2004), p. 1150.

¹⁶D. Vuillaume, C. Boulas, J. Collet, G. Allan, and C. Delerue, *Phys. Rev. B* **58**, 16491 (1998).

¹⁷C. D. Dimitrakopoulos, A. R. Borwn, and A. Pomp, *J. Appl. Phys.* **80**, 2501 (1996).

¹⁸D. Knipp *et al.*, *J. Appl. Phys.* **93**, 347 (2003).

¹⁹M. Shtein *et al.*, *Appl. Phys. Lett.* **81**, 268 (2002).

²⁰B. E. Warren, *X-Ray Diffraction* (Addison-Wesley, Reading, MA, 1969).

²¹The scattered intensity at two monolayers is determined by the relative reflectivities of the substrate and film, and the phase difference between them. These factors determine whether a local minimum or a maximum is obtained (Ref. 14).

²²P. I. Cohen, G. S. Petrich, P. R. Pukite, G. J. Whaley, and A. S. Arrott, *Surf. Sci.* **216**, 222 (1989).

²³H. A. van der Vegt, H. M. van Pinxteren, M. Lohmeier, E. Vlieg, and J. M. C. Thornton, *Phys. Rev. Lett.* **68**, 3335 (1992).

²⁴A. R. Woll, R. L. Headrick, S. Kycia, and J. D. Brock, *Phys. Rev. Lett.* **83**, 4349 (1999).

²⁵G. Ehrlich and F. G. Hudda, *J. Chem. Phys.* **44**, 1039 (1966).

²⁶R. L. Schwoebel and E. J. Chipsey, *J. Appl. Phys.* **37**, 3682 (1969).

²⁷In previous work, we were able to fit data from room-temperature growth on SiO₂ using only two parameters A_1 and A_{pent} (Ref. 13). Refitting the data from (Ref. 13) yields $A_1=A_2=1.0$ and $A_{pent}=0.7$, in agreement with this study.